available at www.sciencedirect.com

ScienceDirect

journal homepage: www.elsevier.com/locate/ejps

Cloning of the pig PEPT2 (pPEPT2) and characterization of the effects of epidermal growth factor (EGF) on pPEPT2-mediated peptide uptake in the renal porcine cell line LLC-PK1

Helle Bach Søndergaard[1], *Silvina A. Bravo*[1,2], *Carsten Uhd Nielsen*, *Sven Frokjaer*, *Birger Brodin*[*]

Molecular Biopharmaceutics Group, Department of Pharmaceutics and Analytical Chemistry, Faculty of Pharmaceutical Sciences, University of Copenhagen, Universitetsparken 2, DK-2100 Copenhagen, Denmark

ARTICLE INFO

Article history:
Received 30 July 2007
Received in revised form
30 November 2007
Accepted 2 January 2008
Published on line 6 January 2008

Keywords:
Pig PepT2
Gly-Sar uptake
LLC-PK1
Epidermal growth factor
Cloning
Proximal kidney cell line

ABSTRACT

The renal di/tri-peptide transporter PEPT2 is situated in the distal parts of the proximal tubule, where it mediates reabsorption of peptides from the primary urine. The transporter has been thoroughly characterised with respect to substrate–affinity relationships, however little is known about its regulation. Previous studies from our group have shown that epidermal growth factor (EGF) down-regulates PepT2 in the rat proximal kidney tubule cell line SKPT0193 cl.2. The aim of the present work was to clone the pig PEPT2 (pPEPT2) and to study the effect of EGF on pPEPT2 expression in the porcine kidney cell line LLC-PK1. pPEPT2 from LLC-PK1 cells was PCR-cloned. The predicted protein consisted of 729 amino acids, had a molecular mass of 81.7 kDa and was 88% identical and 94% similar to hPEPT2, thus displaying a close similarity to the human orthologue. pPepT2 expressing LLC-PK1 cells were cultured in the absence and presence of EGF in the culture media. EGF induced an increase in uptake of ^{14}C-glycylsarcosine ([^{14}C]-Gly-Sar), accompanied by an increase in transcellular electrical resistance, total cell protein, alkaline phosphatase activity and cell density. The increase in uptake of [^{14}C]-Gly-Sar was maximal when cells were cultured in the presence of EGF throughout the culture period of 10 days. The EGF-treatment did not induce significant changes in pPepT2 mRNA expression, as determined by real-time PCR. The effect of EGF thus appears to be an increase in the number of cells without a loss of differentiation, an effect which is quite different from earlier observations on the SKPT cell line.

1. Introduction

The di/tri-peptide transporter PEPT2 (SLC15A2) is situated in the proximal tubules of the kidney (Daniel et al., 1991; Liu et al., 1995; Boll et al., 1996), in the lung (Groneberg et al., 2001a,b) and in the brain, where the most prominent expression occurs at the choroid plexus (Groneberg et al., 2001a,b; Shen et al., 2004). The physiological function of PEPT2 in kidney is to absorb di/tri-peptides from the ultra filtrate (Frey et al., 2007). Furthermore, several drugs and drug candidates such as β-lactam antibiotics, angiotensin converting enzyme (ACE) inhibitors, the antiviral drug Val-acyclovir and the anticancer drug bestatin (Luckner and Brandsch, 2005; Biegel et al., 2006) are transported via PEPT2. PEPT2 has a structure–affinity

[*] *Corresponding author*. Tel.: +45 35 33 61 40; fax: +45 35 33 60 30.
E-mail address: bbr@farma.ku.dk (B. Brodin).
[1] These authors contributed equally.
[2] Present address: Institute of Pharmaceutical Sciences, ETH Zurich, 8093 Zurich, Switzerland.
0928-0987/$ – see front matter © 2008 Elsevier B.V. All rights reserved.
doi:10.1016/j.ejps.2008.01.001

profile much similar to the intestinal isoform PEPT1, but tends to have a lower maximal capacity, but a higher affinity (Biegel et al., 2006). PEPT2 has been suggested to serve an important role as uptake pathway for peptidomimetic drug compounds in the kidney (Shen et al., 2007). Studies on regulation of PEPT2 activity in the kidney are therefore interesting, both from a physiological and a pharmacokinetic point of view. However, although PEPT2 has been thoroughly characterized in terms of function and substrate affinities (Daniel and Herget, 1997; Biegel et al., 2006), little information is currently available on PEPT2 regulation. Our group previously demonstrated an EGF-mediated PEPT2 decrease in PEPT2 expression in the proximal kidney tubule cell line SKPT0193 cl.2 (SKPT) (Bravo et al., 2004). Epidermal growth factor (EGF) is a 53 amino acid polypeptide secreted predominantly by salivary glands and to a lower level by the kidney. Cell division, DNA synthesis and tissue proliferation have been reported after EGF stimulation. Moreover, EGF is involved in the regulation of several plasma membrane transport proteins, i.e., the glucose transporter GLUT-1, the serotonin transporter and the sodium-phosphate cotransporter NaPi-II_b (Mischoulon et al., 1992; Kekuda et al., 1997; Xu et al., 2003) and the intestinal peptide transporter hPEPT1 (Nielsen et al., 2001).

The LLC-PK1 cell line displays morphological characteristics of polarized proximal kidney tubule epithelia. After reaching confluence, they progressively acquire several properties typical of the brush border of the proximal kidney tubules, i.e., alkaline phosphatase and γ-glutamyltranspeptidase activity and the expression of transport systems, e.g., the Na^+-dependent hexose transporter (Sun et al., 1998). Functional evidence, e.g., high-affinity substrate uptake, as well as RT-PCR using conserved primers, has indicated the existence of a pig PEPT2 in LLC-PK1 cells (Wenzel et al., 1998). However, the pig PepT2 gene nucleotide sequence has not been identified previously.

The aim of the present work was to clone pPEPT2 and to investigate whether EGF is involved in PepT2 regulation in the LLC-PK1 cell line. We PCR-cloned pPEPT2 from LLC-PK1 cell lysate and identified the coding sequence of pPepT2. pPEPT2 showed 94% similarity to its human orthologue hPEPT2, thus having a closer resemblance than rodent transporters.

EGF long-term treatment showed increased PEPT2-mediated transport capacity, however no changes were observed in the PepT2 mRNA expression levels after EGF stimulation. This indicates that EGF increases peptide uptake capacity simply by increasing the number of cells per area. Thus EGF does not appear to affect pPEPT2 activity directly, and the effects of EGF on PEPT2 in the LLC-PK1 cell line differs drastically from the effects observed on the SKPT0193 cl.2 cell line.

2. Materials and methods

2.1. Materials

LLC-PK1 cells were obtained from European Collection of Cell Cultures (ECACC, Salisbury, UK). Cell culture media, Hanks' balanced salt solution (HBSS) and human recombinant EGF were purchased from Life Technologies (Taastrup, Denmark). Alexa 488-conjugated phalloidin and propidium iodide were supplied by Molecular Probes (Eugene, Oregon, USA). [^{14}C]-glycylsarcosine ([^{14}C]-Gly-Sar) with a specific activity of 49.94 mCi mmol^{-1}, [^{3}H]-mannitol with a specific activity of 51.50 mCi mmol^{-1} were obtained from New England Nuclear (Boston, Massachusetts, USA) All other chemicals were purchased from Sigma (Saint Louis, Missouri, USA), unless otherwise stated.

2.2. Cell culture

LLC-PK1 cells were received at passage 196 and passaged in 1:1 Dulbecco's modified eagle medium (DMEM)/nutrient mixture F-12 (F12) with L-glutamine, 15 mM *N*-[2-hydroxyethyl]piperazine-*N*′-[2-ethanesulfonate] (HEPES) and piridoxine. The culture media were supplemented with 10% fetal bovine serum, 100 U ml^{-1} penicillin and 100 μg ml^{-1} streptomycin. Stock cells were sub cultured every 7 days by treatment with 0.25% trypsin and 1 mM EDTA in phosphate buffered saline (PBS). Cells at passages 198–210 were seeded onto tissue culture treated Transwells (1 cm^2, 0.4 μm pore size) (Costar, Cambridge, Massachusetts, USA) at a density of 5×10^4 cells cm^{-2}. For some experiments, LLC-PK1 cells growth media were supplemented with 10 ng ml^{-1} of EGF. Monolayers were grown in an atmosphere of 5% CO_2–95% O_2 at 37 °C. Growth media were replaced every second day. Transepithelial electrical resistance (TEER) measurements were performed in tissue resistance measurement Endohm chambers with EVOM volt-ohmmeter, from World Precision Instruments (Sarasota, Florida, USA).

2.3. RNA isolation, quantification and reverse transcription

RNA from LLC-PK1 cells grown throughout a 10 days culture period in the absence or presence of 10 ng ml^{-1} EGF was isolated using the RNeasy Plus Kit (Qiagen AB, Ballerup, DK) as described by the manufacturer. Spectrophotometric measurements of RNA concentration and purity were performed, and only RNA with a 260/280 nm absorbance ratio of 1.8–2.0 was used. Reverse transcription was performed on 2.0 μg RNA with an anchored oligo(dT)primer for first strand cDNA synthesis and the reverse transcriptase Reverse-iT blend from the Reverse-iT Kit (ABgene, Epsom, UK). Each tube with a final volume of 20 μl was incubated at 47 °C for 60 min for efficient first strand synthesis followed by inactivation of the enzyme at 75 °C for 10 min. The cDNA was diluted to a concentration of 10 ng μl^{-1} and stored at −20 °C for later use.

2.4. PCR cloning of pPepT2

Primers covering the putative coding region of pPepT2 were 1F [5′-AAGGAGCCAGCCATGAATCC] (sense) and 2R [5′-AGTCATTAGAGCTTTGTCTTC] (anti-sense). The sense primer, covering the start codon, was determined from homology searches between human, mouse and rat PepT2. The anti-sense primer, covering the stop codon, was determined from homology between hPepT2 and a clone with a partial mRNA from a porcine EST library constructed from embryos (GenBank accession no. CN155883). PCR with these primers

on LLC-PK_1 cDNA gave an amplicon of the expected size at approx. 2200 nucleotides. PCR amplifications were performed in a total volume of 25 μl, containing 125 ng LLC-PK_1 cDNA, 10 × PCR buffer, 2.0 mM $MgCl_2$, 200 μM of each dNTP, 0.2 μM of each primer, and 1 unit Platinum *Taq* DNA polymerase (Invitrogen, Høje Tåstrup, DK). PCR conditions were hotstart at 95 °C for 30 s, followed by 36 cycles of denaturation at 95 °C for 30 s, annealing at 62 °C for 30 s and extension at 72 °C for 1 min 30 s. This was followed by a final 7 min extension. PCR reagents were purchased from ABgene. PCR reactions were performed in a Thermo cycler (MJ Research, PTC-200, Peltier Thermal Cycler) and amplicons were separated on a 1% MetaPhor agarose gel (Cambrex, Glostrup, DK) and visualized by staining with ethidiumbromide (EtBr) (VWR, Albertslund, DK). Images were obtained and analysed on a Kodak Image Station 1000 (Kodak, Rochester, NY, USA). Primer 1F and 2R were purchased from DNA Technology A/S (Aarhus, DK) and used for sequencing of the PCR-cloning amplicon on sense and anti-sense strands (MWG—Biotech AG, Martinsried, Germany). Additional sequencing primers were synthesized at MWG in order to cover the coding region of pPepT2: 4R [5′-TTGGTTGCTCTGGATTCTGC] (anti-sense), 6F [5′-GACTGCTACGCATTGGCTTTTG] (sense), 7R [5′-ATGCTCAATGGATAGTTGG] (anti-sense), 8R [5′-CAGCACAGCTTTCATGCC] (anti-sense) and 9F [5′-GTTTGTTATTACTAATAGC] (sense).

2.5. 5′-RACE (rapid amplification of cDNA ends)

RNA from LLC-PK_1 cells was isolated as described above and 1 μg RNA was reverse transcribed with Superscript III RTase (Invitrogen, Høje Tåstrup, DK) at 55 °C for 60 min, using the gene specific pPepT2 primer: GSP1 [5′-TTGGTTGCTCTGGATTCTGC] (anti-sense). Excess primers and nucleotides were removed with a centricon-100 microconcentrator spin column (Millipore A/S, Copenhagen, DK) and the purified cDNA was tailed with dATP at the 3′-end of the anti-sense strand with terminal transferase (New England Biolabs) at 37 °C for 15 min. The dA-tailed cDNA was then diluted to 500 μl and subsequently 2 μl were used as template for PCR amplification. Primer concentrations used were 0.6 μM of the gene specific pPepT2 primer: GSP2 [5′-CACTCCAATGCAGGAAATACAG] (anti-sense) and 0.6 and 0.3 μM of the two adaptor primers adaptorHBS [5′-GACTCGAGTCGACATCG] (sense) and (dT)17 adaptorHBS [5′-GACTCGAGTCGACATCGATTTTTTTTTTTTTTTTT] (sense), respectively. PCR amplifications were performed in a total volume of 25 μl, containing LLC-PK_1 cDNA, 10 × PCR buffer, 2.0 mM $MgCl_2$, 200 μM of each dNTP and 1 unit HotStar Taq DNA polymerase (Qiagen). PCR conditions were hotstart at 95 °C for 10 min, followed by 1 cycle of denaturation at 94 °C for 5 min, annealing at 55 °C for 5 min and extension at 72 °C for 40 min, followed by 32 cycles of denaturation at 94 °C for 40 s, annealing at 55 °C for 40 s and extension at 72 °C for 1 min. This was followed up by a 10 min final extension. Amplicons were separated on a 3% MetaPhor agarose gel (Cambrex, Glostrup, DK). The amplicon was excised from the gel purified and used for a subsequent secondary PCR with optimized annealing temperature only containing the adaptorHBS and GSP2 primers. PCR conditions for the secondary PCR were: hotstart at 95 °C for 15 min, followed by 35 cycles of denaturation at 95 °C for 18 s, annealing at 58 °C for 30 s and extension at 72 °C for 1.30 min, followed by a 7-min extension at 72 °C. Amplicons were separated on a 1% MetaPhor agarose gel and aliquots were sequenced at MWG (MWG—Biotech AG, Martinsried, Germany).

2.6. Real-time PCR

Real-time PCR amplifications were performed in a total volume of 50 μl, containing 25 ng cDNA, 0.1–0.3 μM of each primer and SYBR® green PCR Master Mix containing AmpliTaqGold and the passive reference ROX (Applied Biosystems, Foster City, CA, USA). Experiments were performed 5–6 times, each in triplicates and in three passages. Non-template controls were included. Reaction parameters were: 10 min at 95 °C, followed by 38 cycles of amplifications (1 min at 60 °C and 20 s at 95 °C). Amplification was followed by melting curve dissociation analysis showing the presence of a single amplicon at 77.5 °C, using an ABI GeneAmp 5700 sequence detection system (Applied Biosystems, Foster City, CA, USA). pPepT2 amplification primers were: [5′-ATCCATTGAGCATTGCCTTC] (sense) and [5′-CACTCCAATGCAGGAAATACAG] (anti-sense), amplicon length was 111 bp. pGAPDH amplification primers were: [5′-AATCCCATCACCATCTTCCA] (sense) and [5′-CATGGTCGTGAAGACACCAG] (anti-sense), amplicon length was 102 bp. Primers were designed to span introns, as estimated from the human isotype, to eliminate signal from any residual contaminating genomic DNA. The expression of pPepT2 in EGF-treated cells compared to control was investigated by the comparative C_T method, also named $\Delta\Delta C_T$ (for detailed description of the $\Delta\Delta C_T$ method, see Applied Biosystems, Guide to Performing Relative Quantitation of Gene Expression Using Real-Time Quantitative PCR).

To validate that target gene and reference gene have the same PCR efficiency, a validation experiment was performed. Of the two reference genes tested, pGAPDH had close to 100% amplification efficiency compared with pPepT2, with a slope of −0.003 in a ΔC_T versus log input semi-log regression line (passes if slope is <0.1) (data not shown). The amount of pPepT2, normalised to pGAPDH and relative to the calibrator, in this case the untreated sample, is given by $2^{-\Delta\Delta C_T}$.

2.7. Glycylsarcosine uptake experiments

Uptake of [^{14}C]-Gly-Sar was measured in HBSS or in standard Krebs' Ringer solution (137 mM NaCl, 5.4 mM KCl, 2.8 mM $CaCl_2$, 0.99 mM $MgSO_4$, 0.34 mM KH_2PO_4, 0.3 mM Na H_2PO_4, 10 mM Glucose) and Na^+-free Krebs' Ringer solution (prepared by replacing NaCl with equimolar choline chloride and omission of NaH_2PO_4), all supplemented with 0.05% bovine serum albumin (BSA). Apical media were buffered with 10 mM 2-(*N*-morpholino)ethanesulfonic acid (MES) and pH was adjusted to 6.0. Basolateral media were buffered with 10 mM HEPES and adjusted to pH 7.4. Cells were placed on a shaking plate, pre-heated to 37 °C and allowed to equilibrate for 15 min in apical and basolateral buffer solutions. The experiment was started by adding fresh apical buffer containing the relevant Gly-Sar concentration and 0.5 μCi [^{14}C]-Gly-Sar per well. In certain experiments, 0.5 μCi [^{3}H]-mannitol per well was added to

the apical solution, as a marker of extracellular space. Pilot studies (data not shown) showed that uptake over time was linear at least up till 60 min at an apical Gly-Sar concentration of 520 μM, in both control cells and cells treated with EGF. In the present study, uptake experiments were terminated after 20 min, unless otherwise stated, by gentle suction of the uptake medium, followed by four washes of the monolayers with ice-cold HBSS. The filters were cut out from the supports and placed in scintillation vials. Radioactivity was determined in a Packard TriCarb liquid scintillation counter, using Ultima Gold scintillation fluid (Canberra Packard).

2.8. Kinetic analysis

Uptake of Gly-Sar as a function of apical Gly-Sar concentration was fitted to a Michaelis–Menten type equation (Eq. (1)):

$$V = \frac{V_{max} \cdot [S]}{K_m + [S]} \quad (1)$$

where V is the flux at substrate concentration [S], K_m the Michaelis–Menten constant and V_{max} is the maximal flux rate.

The ED_{50} value for EGF-mediated stimulation of Gly-Sar uptake was determined using the four-parameter logistic equation (Eq. (2)):

$$R = R_{Max} \frac{R_{Max} - R_{Min}}{1 + 10^{(\log EC_{50} - X)^n}} \quad (2)$$

where R (response) is the flux at a given EGF-concentration, R_{Max} the maximal flux (at [EGF] = 0), R_{Min} the minimal flux (at [EGF] = ∞), X the logarithm of the concentration, and n is the Hill coefficient.

2.9. Total protein content and alkaline phosphatase activity determination

Filters were placed in NP-40 lysis buffer (10 mM Tris·HCl, pH 7.4, 0.25 M sucrose, 1 mM EDTA, 1 mM EGTA, 2% NP-40) in Eppendorf tubes. Cells were removed from the filters by a gentle treatment with a pistil. The tubes were centrifuged at 10 000 × *g* for 10 min. The protein content and the alkaline phosphatase activity were determined in lysates free of cellular debris. Total protein content was determined by the method of Bradford (1976), using the Bio-Rad Protein Assay Kit according to the manufacturers' instructions (Bio-Rad, Hemel Hempstead, UK). Alkaline phosphatase activity was determined by a modification of the Bessey–Lowry–Brock method. The reaction was initiated by adding 0.5 ml of a solution of *p*-nitrophenyl phosphate (1 mg ml^{-1}) prepared in 0.1 M glycine buffer (containing 1 mM $MgCl_2$ and 1 mM $ZnCl_2$, pH 10.4) to 50 μl of cell lysates. After 15 min of incubation at 37 °C, it was stopped by the addition of 138 μl of 3N NaOH. The absorbance of the samples was measured at 405 nm and was compared with the absorbance of standard solutions of *p*-nitrophenol. The alkaline phosphatase unit is defined as the amount of enzyme that liberates 1 μmol *p*-nitrophenol h^{-1}.

2.10. Confocal laser scanning microscopy

Cells grown on filters were fixed for 10 min in HBSS with 3% paraformaldehyde, permeabilized for 5 min in 0.1% Triton X-100 in PBS and blocked for 30 min in a solution of 2% BSA in PBS. Cell morphology was visualized by staining actin filaments with Alexa 488-conjugated phalloidin and cell nuclei with propidium iodide, both from Molecular Probes (Eugene, OR, USA). The cells were incubated with Alexa 488-conjugated phalloidin (1 UI in 200 μl of PBS + 2% BSA) for 30 min, treated with 100 μg ml^{-1} RNAse in 2XSSC buffer solution (300 mM NaCl, 30 mM sodium citrate, pH 7.0) for 20 min and counterstained with 0.5 μM propidium iodide in 2 × SSC buffer solution for 5 min. All preparation steps were performed at room temperature. After washing in 2 × SSC, filters were mounted on coverslips and confocal imaging was performed on a Zeiss LSM 510 confocal laser scanning microscope, using a Zeiss plan apochromat 63× oil immersion objective with a numerical aperture of 1.4. Fluorophores were excited using an argon laser line at 488 nm and a HeNe laser line at 543 nm.

2.11. Statistical analysis

Values are given as mean ± S.E. The statistical significance of the results was determined using a two-tailed Students' *t*-test, or an ANOVA test, when appropriate. $P < 0.05$ was considered significant. *n* refers to the number of cell passages used. $^{*}P < 0.05$, $^{**}P < 0.01$, $^{***}P < 0.001$.

3. Results

3.1. cDNA sequence and protein structure of pPepT2

We have identified the coding sequence of pig PepT2 cDNA by PCR cloning in LLC-PK1 cells followed by subsequent sequencing. The identified pPepT2 sequence was 2222 nucleotides (nt) long and contains an open reading frame of 2190 nt (including termination codon) that encodes a 729 amino acid protein (Fig. 1.) An additional 27 nt were identified upstream from the translation start by 5′-RACE. The cDNA sequence has been deposited in the GenBank (accession number: EF527255). The predicted protein has a molecular mass of 81.7 kDa and is 88% identical and 94% similar to hPEPT2. The pPEPT2 protein has a cytosolic N-terminus and 11 putative transmembrane segments (as predicted by the TMHMM algorithm). A large extracellular loop is located between TMS 9 and 10 and two putative N-glycosylation sites are predicted within this loop at position Asn435 and Asn472. According to TMHMM topology prediction, cytosolic sites accessible to phosphorylation by PKC are Ser28, Ser239, Ser285 and Thr375 (Blom et al., 2004).

3.2. Long-term treatment with EGF stimulates peptide transporter activity in LLC-PK1 cells and causes increased TEER, alkaline phosphatase activity and total cell protein

Apical uptake of radiolabelled Gly-Sar (20 μM) was investigated in LLC-PK1 cells grown in the absence or presence of 10 ng ml^{-1} EGF in both apical and basolateral culture media.

```
pPEPT2       1 MNPFQKNESKETLFLPVSTEEVPPRPPSFPKKPSPKICGSNYPLSIAFIV    50
               |||||||||||||||.|||.|||||||||.|||||||.|||||||||||||||
hPEPT2       1 MNPFQKNESKETLFSPVSIEEVPPRPPSPPKKPSPTICGSNYPLSIAFIV    50

pPEPT2      51 VNEFCERFSYYGMKAVLTLYFLYFLHWSEDTSTSVYHAFSSLCYFTPILG   100
               |||||||||||||||||.|||||||||:||||||:|||||||||||||||||
hPEPT2      51 VNEFCERFSYYGMKAVLILYFLYFLHWNEDTSTSIYHAFSSLCYFTPILG   100

pPEPT2     101 AAIADSWLGKFKTIIYLSLVYVLGHVIKSLGALPILGGHMIHTILSMVGL   150
               ||||||||||||||||||||||||||||||||||||||.::||:||::||
hPEPT2     101 AAIADSWLGKFKTIIYLSLVYVLGHVIKSLGALPILGGQVVHTVLSLIGL   150

pPEPT2     151 SLIALGTGGIKPCVAAFGGDQFEEKHAEERTRYFSVFYLSINAGSLISTF   200
               ||||||||||||||||||||||||||||||||||||||||||||||||||||
hPEPT2     151 SLIALGTGGIKPCVAAFGGDQFEEKHAEERTRYFSVFYLSINAGSLISTF   200

pPEPT2     201 VTPMLRGDVQCFGKDCYALAFGVPGMLMIIALVVFSMGSKIYKKPPPEGN   250
               :||||||||||||:||||||||||:||:||||||:||||||.|||||||
hPEPT2     201 ITPMLRGDVQCFGEDCYALAFGVPGLLMVIALVVFAMGSKIYNKPPPEGN   250

pPEPT2     251 IVTQVVRCIWFAISNRFKNRSGDIPKREHWLDWASEKYSKQLIMDVKALT   300
               ||.||.:|||||||||||||||||||:||||||:|||.||||||||||||
hPEPT2     251 IVAQVFKCIWFAISNRFKNRSGDIPKRQHWLDWAAEKYPKQLIMDVKALT   300

pPEPT2     301 RILFLYIPLPMFWALLDQQGSRWTLQATRMNGNLGFFVLQPDQMQVLNPF   350
               |:|||||||||||||||||||||||||.|||.||||||||||||||||||.
hPEPT2     301 RVLFLYIPLPMFWALLDQQGSRWTLQAIRMNRNLGFFVLQPDQMQVLNPL   350

pPEPT2     351 LVLIFIPLFDLVVYRLVAKCGINFTSLRKMAVGMILACLAFAVAAAVEIK   400
               ||||||||||.|:||||:||||||:||||||||||||||||||||||||||
hPEPT2     351 LVLIFIPLFDFVIYRLVSKCGINFSSLRKMAVGMILACLAFAVAAAVEIK   400

pPEPT2     401 INGMAPPQPDSQEGFLQVLNLANDEVKVTVLGNENSSLLEESIKSFQTMP   450
               ||.|||.||..||.||||||||:||||||||:||||:|||.|||||||..|
hPEPT2     401 INEMAPAQPGPQEVFLQVLNLADDEVKVTVVGNENNSLLIESIKSFQKTP   450

pPEPT2     451 HYSKLHLKTKREDFHFQLKYHNLSVYTEHSVEEKKLYTLIIREDGKSISS   500
               ||||||||||.:||||.|||||||:|||||||:||..|:|:|||||.||||
hPEPT2     451 HYSKLHLKTKSQDFHFHLKYHNLSLYTEHSVQEKNWYSLVIREDGNSISS   500

pPEPT2     501 MMVKDAESRATNGMTAMRFVNTLHEEVNISLGTDTSFSVGKDYGVSAYRT   550
               |||||.|||.|||||.:|||||||::|||||.||||.:||:|||||||||
hPEPT2     501 MMVKDTESRTTNGMTTVRFVNTLHKDVNISLSTDTSLNVGEDYGVSAYRT   550

pPEPT2     551 VQRGEYPVVHCRTKDENFSLNLGLLDFGAAYLFVITNSTGQGPRVQKIEY   600
               |||||||.|||||:|:||||||||||||||||||||:|.||.:..|||.
hPEPT2     551 VQRGEYPAVHCRTEDKNFSLNLGLLDFGAAYLFVITNNTNQGLQAWKIED   600

pPEPT2     601 TPANKMSIAWQLPQYALVTAGEVMFSVTGLEFSYSQAPSSMKSVLQAAWL   650
               .||||||||||||||||||||||||||||||||||||.||||||||||||
hPEPT2     601 IPANKMSIAWQLPQYALVTAGEVMFSVTGLEFSYSQAPSGMKSVLQAAWL   650

pPEPT2     651 LTVAVGNIIVLIVAQFSGLVQWAEFILFSCLLLVVCLIFSIMGYYYIPIK   700
               ||:||||||||:||||||||||||||||||||:||||||||||||:|:|
hPEPT2     651 LTIAVGNIIVLVVAQFSGLVQWAEFILFSCLLLVICLIFSIMGYYYVPVK   700

pPEPT2     701 PEDIQGSADKQIPQIQGNMINLETKKTKL    729
               .||::|.|||.||.|||||||.||||||||
hPEPT2     701 TEDMRGPADKHIPHIQGNMIKLETKKTKL    729
```

Fig. 1 – Amino acid sequence of the predicted pPEPT2 protein aligned with hPEPT2 (multiple sequence alignment ClustalW). The predicted pPEPT2 amino acid sequence is 88% identical and 94% similar to hPEPT2. The sequence can be retrieved in GenBank (accession number: EF527255).

Uptake experiments were performed using either 20 or 40 min of incubation.

Apical uptake rate of 20 μM [^{14}C]-Gly-Sar was followed over a time period of 14 days after seeding the cells (Fig. 2A). LLC-PK1 cells grown in the absence or presence of EGF showed a similar increase in the [^{14}C]-Gly-Sar uptake rate during the first 6 days in culture, but on day 8 and throughout the remaining part of the culture the EGF-treated cells displayed a significantly higher peptide uptake activity ($P < 0.05$, $n = 3$) (Fig. 2A). The [^{14}C]-Gly-Sar uptake rate in LLC-PK1 cells grown in the absence or presence of EGF was 1.35 ± 0.12 and 4.16 ± 0.26 pmol cm^{-2} min^{-1} ($P < 0.001$, $n = 3$), when measured in cells cultured for ten days. The EGF-treatment also caused an increase in the TEER (Fig. 2B). TEER increased gradually during the first 6 days of growth in EGF-treated cells, after which a plateau with significantly higher values for EGF-treated

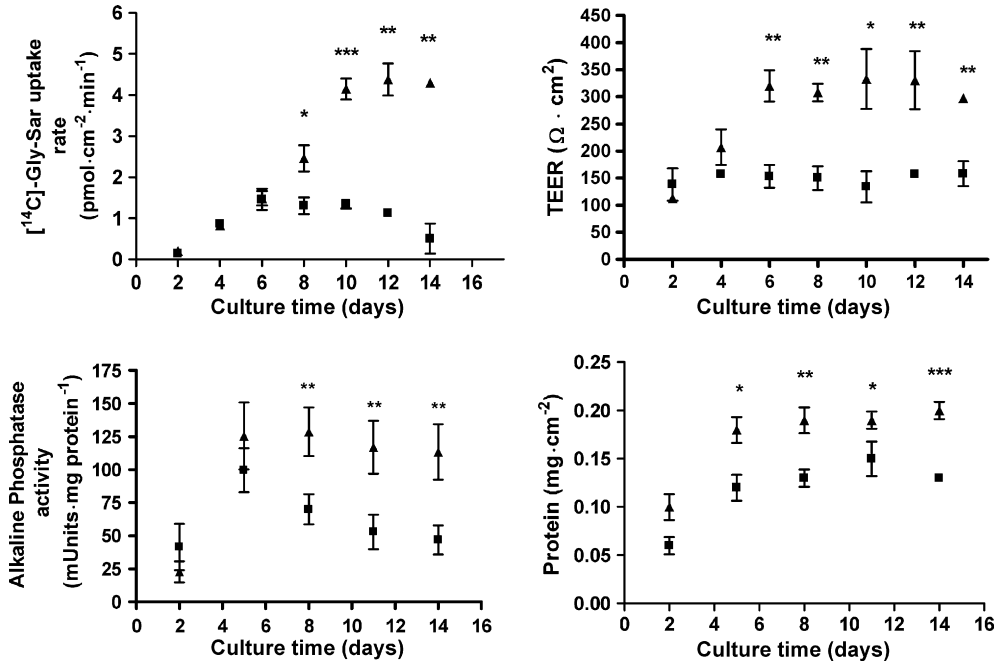

Fig. 2 – LLC-PK1 cell monolayers were grown in the absence (■) or presence (▲) of 10 ng ml^{-1} EGF in the culture media. Experiments were performed in triplicate within each passage, each data point represents mean ± S.E. of at least three individual passages. Values marked by asterisks were significantly higher than the corresponding controls (cells grown in the absence of EGF). $^{*}P < 0.05$; $^{**}P < 0.01$; $^{***}P < 0.001$. (A) Apical uptake rate (measured over 20 min) of [^{14}C]-labelled Gly-Sar at a total Gly-Sar concentration of 20 μM. (B) TEER measured in tissue resistance measurement chambers filled with HBSS at room temperature. (C) Alkaline phosphatase activity measured as release rate of *para*-nitrophenol and normalised with respect to cell protein. (D) Total cell protein measured using the Bradford assay.

cells than those found in non-treated cells was observed ($P < 0.05$, $n = 3$). The TEER was 134 ± 17 and 333 ± 40 Ω cm^2 in LLC-PK1 cells grown for 10 days in the absence and presence of EGF, respectively ($P < 0.05$, $n = 3$). Furthermore, an increase in the differentiation marker enzyme alkaline phosphatase (Fig. 2C) and an increase in total cell protein per area of filter (Fig. 2D) was found. At day 14 of culture alkaline phosphatase activity was 52 ± 12 mUnits (mg protein)$^{-1}$ in controls and 117 ± 20 mUnits (mg protein)$^{-1}$ in EGF-treated cells, respectively ($P < 0.05$, $n = 4$). After 14 days in culture the total protein content was 0.11 ± 0.01 mg cm^{-2} in controls and 0.18 ± 0.01 mg cm^{-2} in LLC-PK1 cells grown in presence of EGF ($P < 0.05$, $n = 7$).

3.3. *EGF increased the cell number per area of the LLC-PK1 cell monolayers*

The morphology of the LLC-PK1 cells grown in the absence or presence of 10 ng ml^{-1} EGF during 10 days was studied by labelling the cell nuclei with propidium iodide and the actin filaments with Alexa fluor 488-conjugated phalloidin (Fig. 3). The vertical scans denoted the formation of monolayers when grown onto polycarbonate filters in both groups of cells. However, LLC-PK1 cells grown in the presence of EGF appeared to form monolayers with higher cell density (204 ± 10 cells/~20 000 μm^2), when compared to cell monolayers grown in the absence of the supplement (170 ± 11 cells/~20 000 μm^2), corresponding to a 20% increase in cell number.

3.4. *EGF stimulation of peptide transporter activity was dose dependent*

The LLC-PK1 cells were grown in media with varying concentrations of EGF (0–50 ng ml^{-1}) throughout a culture period of 10 days. The apical uptake rate of 20 μM of [^{14}C]-Gly-Sar was measured over 20 min of incubation. Apical [^{14}C]-Gly-Sar uptake rate was stimulated by EGF in a dose-dependent manner (Fig. 4A and B). The maximal EGF-induced uptake rate was 3.60 ± 0.43 pmol cm^{-2} min^{-1} ($n = 3$), as compared to the control value of 1.20 ± 0.18 pmol cm^{-2} min^{-1} ($n = 3$). The ED_{50} for the EGF-mediated effect on apical Gly-Sar uptake rate in LLC-PK1 cells was estimated to 0.78 ± 0.54 ng ml^{-1} ($n = 3$) using Eq. (2) (Fig. 4B).

3.5. *The effect of EGF was mediated via basolateral receptors and was maximal when EGF was present throughout the culture period*

In order to investigate functional receptor localization, LLC-PK1 cells were cultured in the presence of 10 ng ml^{-1} EGF in either the apical or basolateral solution, or bilaterally. The uptake rate of 20 μM [^{14}C]-Gly-Sar was measured 10 days after seeding. Although an effect of apical treatment was observed,

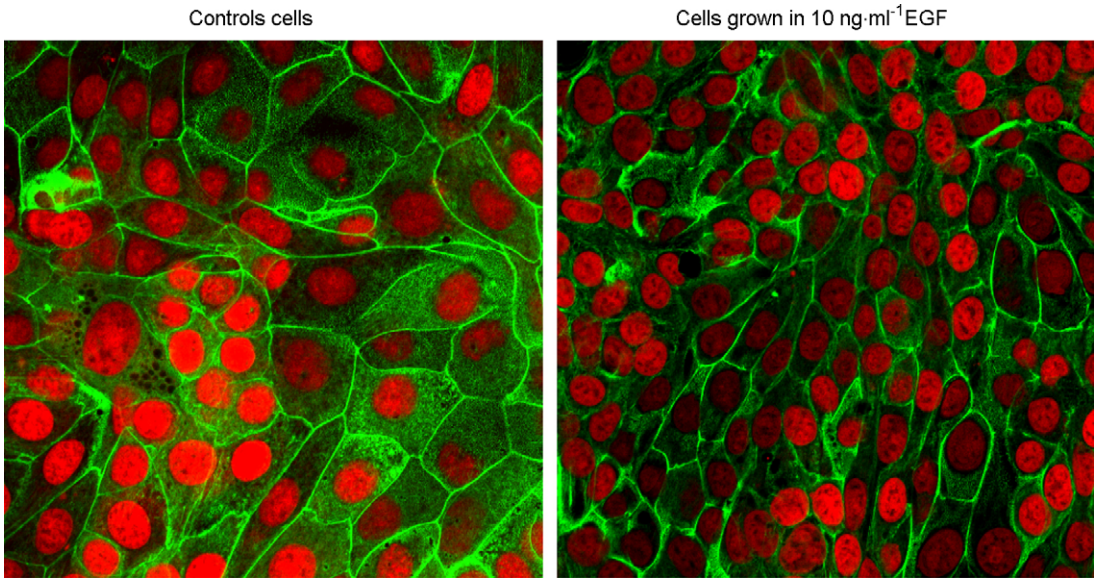

Fig. 3 – LLC-PK1 cells cultured in the absence and presence of 10 ng ml^{-1} EGF for 10 days. After fixation and permeabilization, the LLC-PK1 cells were treated with Alexa 488-conjugated phalloidin (green signal), which visualizes the actin filaments. The cell nuclei were stained with propidium iodide (red signal). Horizontal section of LLC-PK1 cells grown in the absence (left) and presence (right) of EGF. The images are representative of nine preparations, performed in three different cell passages ($n = 3$) (For interpretation of the references to colour in this figure legend, the reader is referred to the web version of the article.).

basolateral treatment induced the largest response (Fig. 4C). At different time points during the culture 10 ng ml^{-1} EGF was added to the growth media in order to investigate the effects on the [^{14}C]-Gly-Sar uptake rate. The Gly-Sar uptake rate was found to increase as the culture time with EGF present increased. The maximal effect was observed when monolayers were exposed throughout the culture period (Fig. 4D).

3.6. *EGF increases the carrier-mediated peptide transport activity*

Apical uptake rate of [^{14}C]-Gly-Sar was measured over a concentration range of 30–520 μM Gly-Sar in LLC-PK1 cells treated throughout the 10 days culture period with 10 ng ml^{-1} EGF and in non-treated cells (Fig. 5A). The obtained values for Gly-Sar uptake rate were corrected for Gly-Sar present in the extra-cellular fluid using the extra-cellular space marker [^{3}H]-mannitol. The corrected data were fitted to the Michaelis–Menten equation, and kinetic constants were calculated. The apparent K_m values for Gly-Sar were 137 ± 11 and 135 ± 39 μM ($P > 0.05$, $n = 6$) for non-treated and EGF treated LLC-PK1 cells, respectively. The maximal capacity of PepT2 was, however, higher in LLC-PK1 cells grown in media containing 10 ng ml^{-1} EGF than in cells grown in EGF-free media (21.4 ± 2.2 pmol cm^{-2} min^{-1} versus 9.3 ± 0.7 pmol cm^{-2} min^{-1}, $P < 0.05$, $n = 6$). In order to confirm that the Gly-Sar uptake was carrier-mediated, apical uptake of [^{14}C]-Gly-Sar was estimated in the absence or presence of the competitive inhibitor Gly-Pro (20 mM) in LLC-PK1 cells grown for 10 days in media containing EGF and in EGF-free media. The apical uptake rate of [^{14}C]-Gly-Sar demonstrated that the uptake was carrier mediated (Fig. 5B). The unspecific [^{14}C]-Gly-Sar uptake, measured in the presence of 20 mM Gly-Pro, was approximately the same in EGF-treated and non-treated LLC-PK1 cells ($P > 0.05$, $n = 3$) (Fig. 5B).

3.7. *mRNA expression levels of pPepT2 did not change in response to EGF treatment in LLC-PK$_1$ cells*

LLC-PK1 cells were cultured in media containing 10 ng ml^{-1} EGF or in EGF-free media and the expression of pPepT2 mRNA was determined on day 10 of growth. Real-time RT-PCR analysis of pPepT2 expression levels relative to the endogenous control pGAPDH in treated versus untreated samples showed no significant difference in expression levels (Table 1).

3.8. *Removal of sodium from the apical solution did not influence on the EGF-mediated increase in peptide transporter activity*

EGF might influence the intracellular pH by activation of sodium-proton exchangers. It was therefore investigated whether removal of sodium from the apical solution affected the EGF-induced increase in the peptide uptake rate. Apical uptake rate of [^{14}C]-Gly-Sar was measured in LLC-PK1 cells grown with 10 ng ml^{-1} EGF and in EGF-free media, and in the absence or presence of Na^+ in the buffer solutions. Sodium-free media reduced pPepT2-mediated uptake rate in both controls and EGF-treated cells proportionally (Fig. 6), thereby indicating that apical proton exchangers does not play a role in the EGF-induced increase in [^{14}C]-Gly-Sar uptake rate.

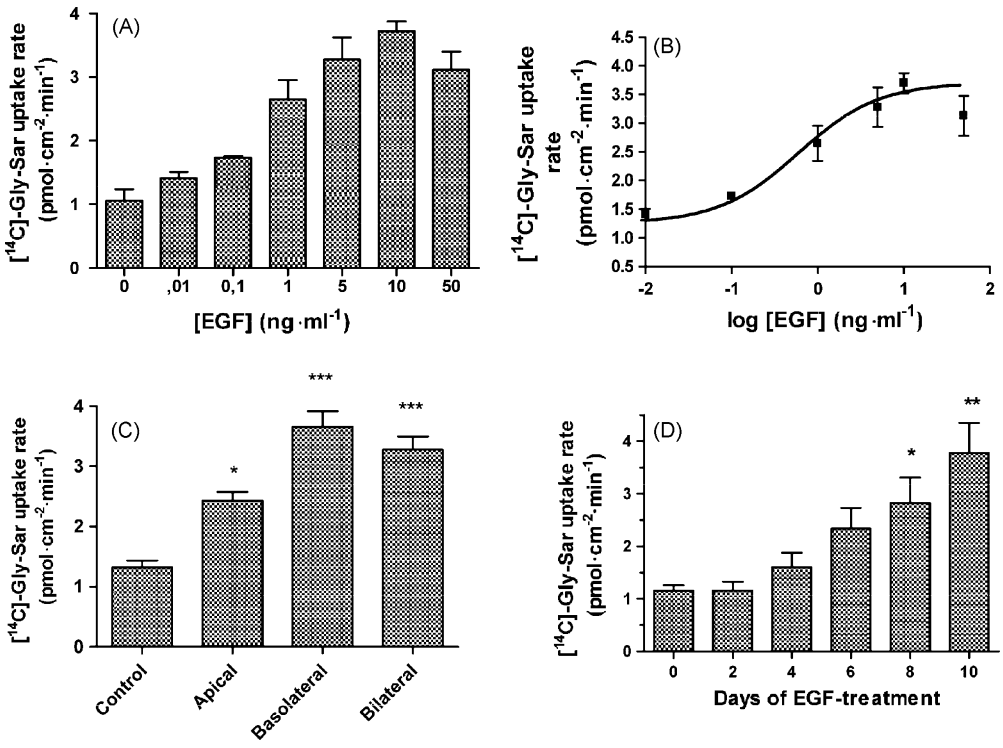

Fig. 4 – (A) Dose dependency of EGF-stimulation. EGF was added bilaterally in varying doses to LLC-PK1 monolayers throughout a culture period of 10 days. At day 10, apical uptake of 20 μM [^{14}C]-Gly-Sar was measured over 20 min. Experiments were performed in triplicate within each passage. Each bar represents mean ± S.E. of three individual passages. Values marked by asterisks were significantly higher than the control (cells cultured in EGF-free media throughout the culture period). $^{*}P < 0.05$; $^{**}P < 0.01$; $^{***}P < 0.001$. (B) Data from (A) were fitted to Eq. (2), the solid line represents the calculated curve fit. (C) EGF-receptor localization. LLC-PK1 cells were grown for 10 days in the absence of EGF, with 10 ng ml^{-1} EGF added apically, basolaterally, or in both apical and basolateral media. At day 10, apical [^{14}C]-Gly-Sar uptake experiments were performed, as described above. (D) Time dependency of EGF stimulation. EGF (10 ng ml^{-1}) was added to the culture media at different time points during the growth period. At day 10 of cell culture, apical uptake of [^{14}C]-Gly-Sar uptake experiments were performed, as described above.

4. Discussion

4.1. *Identification of the porcine PepT2 sequence*

pPepT2 was identified by PCR-cloning and the predicted protein showed great similarity to other species. Analysis by the TMHMM program predicted 11 transmembrane segments (TMS) in pPepT2 resulting in a protein with a N-terminus in the cytosol and an extracellular C-terminus, however, the TMS orientation vary with the different programs used between 10 and 13 TMS and the predicted topology will have to be experimentally determined. It should also be noted that the topology prediction of porcine PEPT1 yields an 11-TMS protein (Klang et al., 2005). pPEPT2 has a potential casein kinase I (CKI) phosphorylation site at Ser18, which is conserved in mouse, rat, rabbit, pig and human. CKI has multiple isoforms and among their diverse functions are regulation of the circadian clock (Partch et al., 2006). However, earlier results have shown that renal rPEPT2 and rPEPT1 only show little change in expression due to diurnal rhythm (Pan et al., 2002). The LLC-PK1 cell line originates from pig and has thus an advantage as compared to rat SKPT cells in the study of drug disposition, due to their physical and genetic resemblance to human, as compared to rodent (Chen et al., 2007). However, primary renal cell cultures have been shown to express hPEPT2 (Lash et al., 2006) and they

Table 1 – Real-time RT-PCR of pPepT2 and pGAPDH mRNA-fold change expression of pPepT2 after treatment

LLC-PK1 samples	pPepT2, C_T	pGAPDH, C_T	PEPT2-GAPDH, ΔC_T	ΔC_T treated – ΔC_T untreated, $\Delta\Delta C_T$	Fold difference in pPepT2 relative to untreated, $2^{-\Delta\Delta C_T}$
Untreated	28.6 ± 0.2	19.7 ± 0.2	8.9 ± 0.3	0.0 ± 0.3	1.0 (0.8–1.2)
Treated (10 ng (ml EGF)$^{-1}$)	28.0 ± 0.3	19.1 ± 0.2	8.9 ± 0.4	0.0 ± 0.4	1.0 (0.8–1.3)

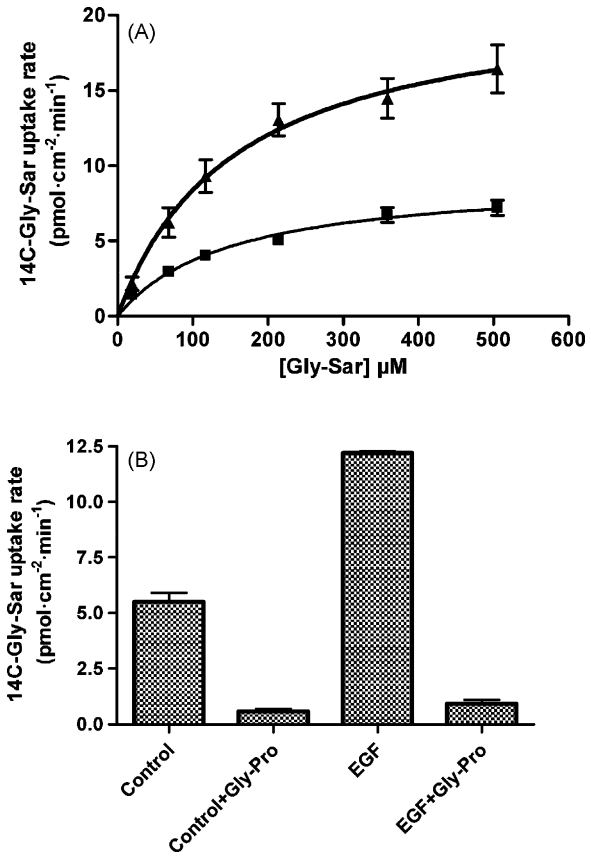

Fig. 5 – (A) Gly-Sar concentration dependence of the apical [^{14}C]-Gly-Sar uptake rate in LLC-PK1 cells grown in the absence (■) or presence (▲) of 10 ng ml^{-1} EGF in the culture media. The apical uptake rate of [^{14}C]-Gly-Sar, at a Gly-Sar concentration range of 30–520 μM was measured over a 40 min incubation period on day 10. The total [^{14}C]-Gly-Sar measured in the LLC-PK1 cell monolayers, was corrected for radiolabel Gly-Sar remaining in the extracellular spaces by using [^{3}H]-mannitol. The corrected data points were fitted to the Michaelis–Menten equation (Eq. (1)), the fit being represented by solid lines. Experiments were performed in duplicate within each passage. Each data point represents the mean ± S.E. of six individual passages. (B) Apical [^{14}C]-Gly-Sar uptake rate in EGF-treated and non-treated LLC-PK1 cells was measured in the absence or presence of 20 mM Gly-Pro in the donor solution. The apical uptake rate of [^{14}C]-Gly-Sar, at a Gly-Sar concentration of 220 μM was determined as described above. The uptake values marked by asterisks, in the absence of Gly-Pro, were significantly higher than those obtained in the presence of Gly-Pro.

might, when further characterized, serve as a tool for analysis of drug disposition and transporter regulation.

We have earlier generated an antibody against the N-terminus (aa 1–15) of ratPEPT2. The pig sequence has a leucine instead of a serine at position 15. Thus the epitope of pPEPT2 is dramatically different from the rat PEPT2, since serine is polar and leucine nonpolar and the loss of a single hydrogen bond at the antigen–antibody interface can reduce the strength of interaction 1000-fold (Harlow and Lane, 1988). Thus, a new

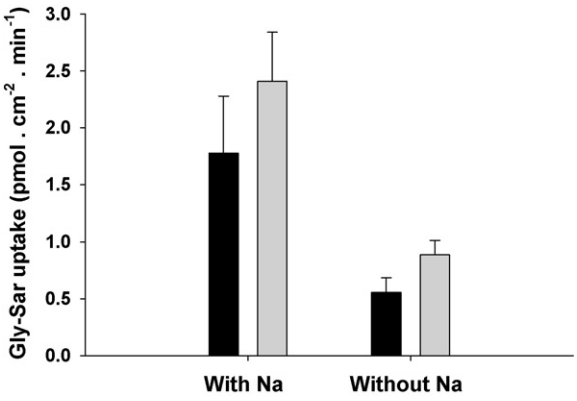

Fig. 6 – Na^{+} dependence of the apical [^{14}C]-Gly-Sar uptake rate in LLC-PK1 cells cultured in the absence (filled bars) and presence (shaded bars) of 10 ng ml^{-1} EGF. The apical uptake of 20 μM [^{14}C]-Gly-Sar was measured over a 20 min incubation period on day 10, using Krebs' Ringer solution containing either Na^{+} or equimolar amount of choline. Experiments were performed in triplicate within each passage. Each bar represents mean ± S.E. of three individual passages.

antibody must be raised, either pPEPT2 specific or against conserved PEPT2 regions, before pPEPT2 protein expression levels can be quantified.

4.2. *EGF increases peptide transport capacity and appears to increase differentiation-specific parameters in the LLC-PK1 cell line*

Only a few studies have demonstrated regulation of PEPT2. Changes in PEPT2 mRNA levels have been observed in rats after nephrectomy (Takahashi et al., 2001; Nakamura et al., 2004). Down-regulation of PEPT2 activity has been shown after phorbol ester treatment in LLC-PK1 cells (Wenzel et al., 1999).

The PDZ containing protein PDZK1 has been shown to enhance PEPT2 transport activity, presumably by influencing subcellular localisation of the transporter (Sugiura et al., 2006). In our previous study, long-term treatment with EGF caused a decrease in rPEPT2 transport capacity in the SKPT cells (Bravo et al., 2004). This effect of EGF was due to a decrease in the rPEPT2 protein expression caused by a decrease in rPEPT2 mRNA.

In the present study we demonstrated that EGF induced up-regulation of PEPT2-mediated transport activity in LLC-PK1 cells. The effect of EGF on the PEPT2 activity was dependent on the EGF concentration and on the stimulation period. EGF, in a concentration of 10 ng ml^{-1} in the cell culture media, increased the V_{max} of the transporter by ~170%, without changing the apparent affinity constant K_m. pPepT2 mRNA expression levels were, however, not significantly modified by EGF treatment in LLC-PK1 cells. Cell differentiation parameters such as alkaline phosphatase activity and TEER were increased after EGF stimulation in the LLC-PK1 cell line. An increase in cell number was also observed. Those results are in accordance with early studies addressing EGF-induced mitogenesis in LLC-PK1 cells at subconfluency (Mullin and McGinn,

1988). In this study the amount of cells per area was increased in about 1.2 times after EGF stimulation. The total protein content values in EGF-treated LLC-PK1 cells are also higher than the values obtained in non-treated ones. This situation differs, however, with that observed in SKPT cells, where the amount of cells per area was increased after EGF treatment, but the total protein content of the monolayers remained unchanged (Bravo et al., 2004).

PEPT2 up-regulation may be caused by an increase in the driving force for peptide uptake in the LLC-PK1 cells. PEPT2, as well as PEPT1, cotransport peptides together with H^+ and therefore the driving force for translocation is partially given by the electrochemical H^+ gradient. Thwaites and co-workers have provided evidence for the functional interaction between hPEPT1 and the Na^+/H^+ exchanger type 3 (NHE3) in the Caco-2 cell line (Kennedy et al., 2002).

NHE3 is expressed in the apical membrane of the LLC-PK1 cells (Shugrue et al., 1999); however, its functional interaction with PepT2 has not been proven. EGF has been reported to be involved in acute regulation of Na^+/H^+ exchangers in various tissues (Takasu et al., 1990; Donowitz et al., 2000). We investigated whether the increase in V_{max} observed in this study was due to an increase in the exchanger activity, which may lead to an increase in the driving force for di-peptide translocation. EGF stimulated Gly-Sar uptake, both in the absence or presence of Na^+, in a proportional manner. This observation, therefore, suggests that the Gly-Sar uptake increase in EGF-treated LLC-PK1 cells is not due to NHE stimulation.

A simple explanation on the increased peptide uptake capacity in LLC-PK1 cells could be that the individual EGF-treated cells retained the same number of transporters per cell as the non-treated cells. The increased number of cells in the EGF-treated monolayers would thus lead to a larger number of transporters per monolayer, and thereby increased peptide uptake capacity. This would also explain the increase in total cell protein and alkaline phosphatase activity. This emphasizes the need of careful analysis of multiple effect parameters, when dealing with agonists with multiple effects, like EGF.

However, this hypothesis does not offer an explanation of the fact that EGF does not down-regulate PEPT2 in LLC-PK1 cells, as it could be expected from earlier studies on EGF-regulation of rPEPT2 (Bravo et al., 2004).

4.3. *Conclusions*

The pPepT2 sequence from the proximal kidney tubule cell line LLC-PK1 was identified, and revealed overall great similarity to hPepT2. The effects of EGF on peptide transport activity, as well as on tissue morphology and differentiation specific parameters, were investigated. Peptide uptake capacity was increased as a consequence of the treatment. It appears that the main effect of EGF in LLC-PK1 cells is proliferative, i.e., causes an increase in cell number per area. EGF does not cause a dedifferentiation and decrease in peptide transporter activity, as previously observed for rPEPT2 in the rat proximal kidney tubule cell line SKPT0193 cl.2 and for hPEPT1 in the intestinal cell line Caco-2. This could be speculated to be due to species differences or differences in the regulatory pathways, presumably the MAPK signalling route, present in the respective cell lines. It thus appears that pPEPT2 in LLC-PK1-cells is not long-term regulated directly by EGF, and since this cell line is likely to have the closest resemblance to the human tissue, it could argue in favour of no direct EGF-regulation in humans. However, *in vivo* studies must be employed, in order to investigate species differences, and the signalling pathways should be analysed using array- and phosphorylation assays, both in cell lines and *in vivo*.

Acknowledgements

The authors appreciate the work of technicians Birgitte Eltong, Susanne Nørskov Sørensen and Bettina Dinitzen. The Carlsberg Foundation and the Novo Nordic Foundation supported the work. The Alfred Benzon Foundation is acknowledged for supporting the research of Silvina A. Bravo.

REFERENCES

Biegel, A., Gebauer, S., Brandsch, M., Neubert, K., Thondorf, I., 2006. Structural requirements for the substrates of the H^+/peptide cotransporter PepT2 determined by three-dimensional quantitative structure–activity relationship analysis. J. Med. Chem. 49, 4286–4296.

Blom, N., Sicheritz-Ponten, T., Gupta, R., Gammeltoft, S., Brunak, S., 2004. Prediction of post-translational glycosylation and phosphorylation of proteins from the amino acid sequence. Proteomics 4, 1633–1649.

Boll, M., Herget, M., Wagener, M., Weber, W.M., Markovich, D., Biber, J., Clauss, W., Murer, H., Daniel, H., 1996. Expression cloning and functional characterization of the kidney cortex high-affinity proton-coupled peptide transporter. Proc. Natl. Acad. Sci. U.S.A. 93, 284–289.

Bradford, M.M., 1976. A rapid and sensitive method for the quantitation of microgram quantities of protein utilizing the principle of protein-dye binding. Anal. Biochem. 72, 248–254.

Bravo, S.A., Nielsen, C.U., Amstrup, J., Frokjaer, S., Brodin, B., 2004. Epidermal growth factor decreases PepT2 transport capacity and expression in the rat kidney proximal tubule cell line SKPT0193 cl.2. Am. J. Physiol. Renal Physiol. 286, F385–F393.

Chen, K., Baxter, T., Muir, W.M., Groenen, M.A., Schook, L.B., 2007. Genetic resources, genome mapping and evolutionary genomics of the pig (*Sus scrofa*). Int. J. Biol. Sci. 3, 153–165.

Daniel, H., Herget, M., 1997. Cellular and molecular mechanisms of renal peptide transport. Am. J. Physiol. 273, F1–F8.

Daniel, H., Morse, E.L., Adibi, S.A., 1991. The high and low affinity transport systems for dipeptides in kidney brush border membrane respond differently to alterations in pH gradient and membrane potential. J. Biol. Chem. 266, 19917–19924.

Donowitz, M., Janecki, A., Akhter, S., Cavet, M.E., Sanchez, F., Lamprecht, G., Zizak, M., Kwon, W.L., Khurana, S., Yun, C.H., Tse, C.M., 2000. Short-term regulation of NHE3 by EGF and protein kinase C but not protein kinase A involves vesicle trafficking in epithelial cells and fibroblasts. Ann. N.Y. Acad. Sci. 915, 30–42.

Frey, I.M., Rubio-Aliaga, I., Siewert, A., Sailer, D., Drobyshev, A., Beckers, J., de Angelis, M.H., Aubert, J., Bar, H.A., Fiehn, O., Eichinger, H.M., Daniel, H., 2007. Profiling at mRNA, protein, and metabolite levels reveals alterations in renal amino acid handling and glutathione metabolism in kidney tissue of PepT2−/− mice. Physiol. Genomics 28, 301–310.

Groneberg, D.A., Doring, F., Nickolaus, M., Daniel, H., Fischer, A., 2001a. Expression of PepT2 peptide transporter mRNA and

protein in glial cells of rat dorsal root ganglia. Neurosci. Lett. 304, 181–184.
Groneberg, D.A., Nickolaus, M., Springer, J., Doring, F., Daniel, H., Fischer, A., 2001b. Localization of the peptide transporter PepT2 in the lung: implications for pulmonary oligopeptide uptake. Am. J. Pathol. 158, 707–714.
Harlow, E., Lane, D., 1988. Antibodies. A Laboratory Manual. Cold Spring Harbor Laboratory Press, Cold Spring Harbor, New York.
Kekuda, R., Torres-Zamorano, V., Leibach, F.H., Ganapathy, V., 1997. Human serotonin transporter: regulation by the neuroprotective agent aurintricarboxylic acid and by epidermal growth factor. J. Neurochem. 68, 1443–1450.
Kennedy, D.J., Leibach, F.H., Ganapathy, V., Thwaites, D.T., 2002. Optimal absorptive transport of the dipeptide glycylsarcosine is dependent on functional Na^+/H^+ exchange activity. Pflugers Arch. 445, 139–146.
Klang, J.E., Burnworth, L.A., Pan, Y.X., Webb Jr., K.E., Wong, E.A., 2005. Functional characterization of a cloned pig intestinal peptide transporter (pPepT1). J. Anim. Sci. 83, 172–181.
Lash, L.H., Putt, D.A., Cai, H., 2006. Membrane transport function in primary cultures of human proximal tubular cells. Toxicology 228, 200–218.
Liu, W., Liang, R., Ramamoorthy, S., Fei, Y.J., Ganapathy, M.E., Hediger, M.A., Ganapathy, V., Leibach, F.H., 1995. Molecular cloning of PEPT 2, a new member of the H^+/peptide cotransporter family, from human kidney. Biochim. Biophys. Acta 1235, 461–466.
Luckner, P., Brandsch, M., 2005. Interaction of 31 beta-lactam antibiotics with the H^+/peptide symporter PepT2: analysis of affinity constants and comparison with PEPT1. Eur. J. Pharm. Biopharm. 59 (1), 17–24.
Mischoulon, D., Rana, B., Kotliar, N., Pilch, P.F., Bucher, N.L., Farmer, S.R., 1992. Differential regulation of glucose transporter 1 and 2 mRNA expression by epidermal growth factor and transforming growth factor-beta in rat hepatocytes. J. Cell Physiol. 153, 288–296.
Mullin, J.M., McGinn, M.T., 1988. Epidermal growth factor-induced mitogenesis in kidney epithelial cells (LLC-PK1). Cancer Res. 48, 4886–4891.
Nakamura, N., Masuda, S., Takahashi, K., Saito, H., Okuda, M., Inui, K., 2004. Decreased expression of glucose and peptide transporters in rat remnant kidney. Drug Metab. Pharmacokinet. 19, 41–47.
Nielsen, C.U., Amstrup, J., Steffansen, B., Frokjaer, S., Brodin, B., 2001. Epidermal growth factor inhibits glycylsarcosine transport and hPepT1 expression in a human intestinal cell line. Am. J. Physiol. Gastrointest. Liver Physiol. 281, G191–G199.
Pan, X., Terada, T., Irie, M., Saito, H., Inui, K., 2002. Diurnal rhythm of H^+-peptide cotransporter in rat small intestine. Am. J. Physiol. Gastrointest. Liver Physiol. 283, G57–G64.
Partch, C.L., Shields, K.F., Thompson, C.L., Selby, C.P., Sancar, A., 2006. Posttranslational regulation of the mammalian circadian clock by cryptochrome and protein phosphatase 5. Proc. Natl. Acad. Sci. U.S.A. 103, 10467–10472.
Shen, H., Smith, D.E., Keep, R.F., Brosius III, F.C., 2004. Immunolocalization of the proton-coupled oligopeptide transporter PepT2 in developing rat brain. Mol. Pharm. 1, 248–256.
Shen, H., Ocheltree, S.M., Hu, Y., Keep, R.F., Smith, D.E., 2007. Impact of genetic knockout of PepT2 on cefadroxil pharmacokinetics, renal tubular reabsorption, and brain penetration in mice. Drug Metab. Dispos. 35, 1209–1216.
Shugrue, C.A., Obermuller, N., Bachmann, S., Slayman, C.W., Reilly, R.F., 1999. Molecular cloning of NHE3 from LLC-PK1 cells and localization in pig kidney. J. Am. Soc. Nephrol. 10, 1649–1657.
Sugiura, T., Kato, Y., Kubo, Y., Tsuji, A., 2006. Mutation in an adaptor protein PDZK1 affects transport activity of organic cation transporter OCTNs and oligopeptide transporter PepT2. Drug Metab. Pharmacokinet. 21, 375–383.
Sun, L., Weaver, D.J., Amsler, K., Weiss, E.R., 1998. Inhibition of cell differentiation by G alpha q in the renal epithelial cell line LLC-PK1. Am. J. Physiol. 274, C1030–C1039.
Takahashi, K., Masuda, S., Nakamura, N., Saito, H., Futami, T., Doi, T., Inui, K., 2001. Upregulation of H^+-peptide cotransporter PepT2 in rat remnant kidney. Am. J. Physiol. Renal Physiol. 281, F1109–F1116.
Takasu, N., Komiya, I., Nagasawa, Y., Asawa, T., Shinoda, T., Yamada, T., Shimizu, Y., 1990. Stimulation of porcine thyroid cell alkalinization and growth by EGF, phorbol ester, and diacylglycerol. Am. J. Physiol. 258, E445–E450.
Wenzel, U., Diehl, D., Herget, M., Daniel, H., 1998. Endogenous expression of the renal high-affinity H^+-peptide cotransporter in LLC-PK1 cells. Am. J. Physiol. 275, C1573–C1579.
Wenzel, U., Diehl, D., Herget, M., Kuntz, S., Daniel, H., 1999. Regulation of the high-affinity H^+peptide cotransporter in renal LLC-PK1 cells. J. Cell Physiol. 178, 341–348.
Xu, H., Inouye, M., Hines, E., Collins, J.F., Ghishan, F.K., 2003. Transcriptional regulation of the human NaPi-II_b cotransporter by EGF in Caco-2 cells involves c-Myb. Am. J. Physiol. 284, C1262–C1271.